ELSEVIER

www.elsevier.nl/locate/jorganchem

Journal of Organometallic Chemistry 607 (2000) 78–92

Journal of Organometallic Chemistry

Novel cationic and neutral Pd(II) complexes bearing imidazole based chelate ligands: synthesis, structural characterisation and catalytic behaviour

Melanie C. Done [a], Thomas Rüther* [a,1], Kingsley J. Cavell* [a,2], Melvyn Kilner [b], Evan J. Peacock [c], Nathalie Braussaud [a], B.W. Skelton [d], Allan White [d]

[a] *Department of Chemistry, University of Tasmania, GPO Box 252-75, Hobart, Tasmania 7001, Australia*
[b] *Department of Chemistry, Cardiff University, PO Box 912, Cardiff CF10 3TB, Wales, UK*
[c] *Central Science Laboratory (CSL), University of Tasmania, GPO Box 252-74, Hobart, Tasmania 7001, Australia*
[d] *Department of Chemistry, University of Western Australia, Nedlands, WA 6907, Australia*

Received 7 March 2000; received in revised form 16 April 2000

Dedicated to Professor Martin Bennett on the occasion of his retirement and in recognition of his major international contribution to organometallic chemistry.

Abstract

A variety of neutral and cationic methyl palladium(II) complexes $[Pd(CH_3)(Cl)(L–L)]$ (**3**) and $[Pd(CH_3)(CH_3CN)(L–L)]BF_4$ (**4**), containing known and new *N*-methylimidazole-2-yl (mim) and *N*-methylbenzimidazole-2-yl (bmim) based chelate ligands (L–L) have been synthesised. The dichloro complexes $[Pd(Cl)_2\{(mim)_2CO\}]$ (**2b**) and $[Pd(Cl)_2(mim)PPh_2]$ (**2e**) have also been synthesised. The crystal structures of $[Pd(Cl)_2\{(mim)_2C{=}NPh\}]$ (**2d**) and $[Pd(CH_3)(Cl)\{(bmim)_2CO\}]$ (**3c**) have been determined and show a square planar geometry at palladium(II) with an appreciable diminished bite angle (85.6°) in **3c** compared to **2d** (88.5°). The molecular structure of **2d** and **3c** show both bisimidazole ligands coordinated via the ring nitrogen donors and inclination of the chelate ring bridge to the coordination plane (boat conformation). Low temperature NMR spectra indicate boat-to-boat inversion of the chelate ring in $[Pd(CH_3)(CH_3CN)\{(mim)_2CO\}]^+$ (**4b**). Examples of the neutral and cationic complexes were tested in the Heck reaction and CO/ethylene copolimerisation respectively. The C=O bridged bisimidazole complex (**3b**) exhibited high activity (TON of 100 000) in the Heck reaction whereas the closely related benzimidazole complex **3c** was about half as active (TON of 53 000). Low activities were found for the cationic complex **4b** in the CO/ethylene copolymerisation (TON 449).

Keywords: Palladium; Imidazole ligands; Heck reaction; CO/ethylene copolymerisation

1. Introduction

Palladium alkyl complexes play an important role in transformation reactions of unsaturated molecules. A key step in these reactions is the insertion into the metal–carbon bond [1]. A number of neutral and cationic Pd complexes [PdRX(L–L)] bearing chelating nitrogen ligands [2] were reported to undergo facile insertion reactions [3] and hence have received significant attention as catalysts for olefin polymerisation [4], olefin/CO copolymerisation [3c,5] and olefin/alkylacrylate copolymerisation [6]. Previous studies have been primarily devoted to complexes incorporating rigid chelating diimine or bipyridine type ligands [3a–c, f–i]. In more recent papers Jordan et al. [7] described neutral and cationic Pd(II) complexes containing bis(pyrazolyl)methane ligands which oligomerise ethylene to predominantly linear internal C_8–C_{24} olefins. Klaeui et al. [8] reported Ni complexes bearing related tris(pyrazolyl)borata ligands which catalyse the ethylene/CO copolymerisation, and Vrieze et al. [3e] investigated Pd complexes containing tridentate nitrogen ligands with varying N-heterocycles.

[1] *Corresponding author.
[2] *Corresponding author. Fax: +61-3-6226-2858; e-mail: cavell-kj@cardiff.ac.uk

0022-328X/00/$ - see front matter
PII: S0022-328X(00)00227-8

Imidazole and benzimidazole ligands [9] have primarily been used to model the binding sites of enzymes in order to provide insight into the nature of enzymatic catalytic cycles [10]. However, very recently the groups of Field and Messerle [11] have studied Rh and Ru complexes of bisimidazole type ligands and investigated the performance of the Rh complexes in intramolecular cyclisation, hydroamination and hydrosilation reactions. Monomethyl and dimethyl Pd(II) complexes of bridged bisimidazole and mixed imidazole–N-heterocycle (py, pz) ligands have been prepared by Canty et al. and their dynamic behaviour has been studied by variable temperature NMR [12].

The strong nucleophilic properties and the bisiimine like structure of bridged bisimidazole chelate ligands led us to investigate several new cationic and neutral Pd(II) complexes of these ligands. Furthermore, the use of complexes of this ligand type had not previously been reported in catalytic carbon–carbon coupling reactions. We were interested in investigating the coordination properties of a series of imidazole based ligands and determine how electronic and steric factors of these ligands influence reactivity at the metal centre. Consequently we have synthesised complexes in which the Pd centre was placed in bisimidazole frameworks with different substitution patterns. We now report the synthesis and first structural characterisation of Pd(II) halogen and methyl complexes bearing functionalised bisimidazole ligands. Their behaviour in the ethylene/CO copolymerisation and the Heck reaction is also reported.

2. Experimental

2.1. General

Solvents were dried and purified by standard methods and freshly distilled under N_2 immediately prior to use. All manipulations were carried out using standard Schlenk techniques or in a nitrogen glovebox. Tetramethyl tin [13], [Pd(Cl)$_2$(COD)] [14], [Pd(Me)(Cl)-(COD)] [15], and ligands **1c** [16], **1e** [17] were prepared according to published procedures. Ligands **1a**,**b**,**d**,**f** were prepared by modified literature procedures or by methods developed in our laboratory. All other reagents were used as received. Nuclear magnetic resonance (NMR) spectra were recorded at ambient temperature (20°C), unless otherwise indicated, on a Varian Gemini-200 NMR spectrometer and on a Varian Unity Inova 400 WB NMR spectrometer. Chemical shifts (δ) are reported in units of ppm relative to internal TMS (^{13}C, ^{1}H), or external 85% H_3PO_4 (^{31}P). Coupling constants (J) are given in Hz and NMR peaks are labelled as singlet (s), doublet (d), triplet (t), quartet (q), multiplet (m) and broad (br). Elemental analysis were recorded by the Central Science Laboratory (CSL), University of Tasmania, on a Carlo Erba EA 1108 elemental analyser. Gas chromatography (GC) was performed on a Hewlett–Packard 5890 series II GC fitted with a SGE 50QC3/BP1 0.5 capillary column and flame ionisation detector (FID). GC-MS and MS were carried out by the CSL, using a HP5890 GC fitted with a 25 m HP1 column (0.32 μm film) and a HP5970B mass selective detector, and a Kratos Concept ISQ MS by liquid secondary ion mass spectrometry (LSIMS, 10 kV caesium ions, *m*-nitrobenzyl alcohol matrix) with an accelerating voltage of 5.3 KV. ESI spectra were recorded on a Finnigan LCQ spectrometer (direct infusion 3 μl min^{-1}, needle voltage 4.5 kV, capillary voltage 20 V, sheath gas 30 psi). Infrared (IR) spectra were recorded on a Bruker IFS-66 FTIR spectrometer.

2.2. Structure determinations

Full spheres of low-temperature CCD area-detector diffractometer data were measured (Bruker AXS instrument; $2\theta_{max} = 58°$, ω-scans; T ca. 153 K; monochromatic Mo–K$_\alpha$ radiation, $\lambda = 0.7107_3$ Å) yielding N_{total} reflections, merging to N unique (R_{int} quoted) after 'empirical'/multiscan absorption correction, N_o with $F > 4\sigma(F)$ being considered 'observed' and used in the full-matrix least-squares refinement, refining anisotropic thermal parameter forms for the non-hydrogen atoms. (x, y, z, and $U_{iso})_H$HH were refined for **2d**, and constrained at estimated values for **3c**. Conventional residuals R, R_w (reflection weights: $(\sigma^2(F) + 0.0004F^2)^{-1}$) are quoted at convergence. Neutral atom complex scattering factors were employed, computation using the XTAL 3.4 program system [31]. Pertinent results are given below and in the Figure and Tables, full atom parameters being deposited.

2.2.1. Crystal/refinement data

2.2.1.1. Compound ***2d***. $C_{15}H_{15}Cl_2N_4Pd$. $CHCl_3$, $M = 562.0$. Monoclinic, space group $P2_1/c$ (C_{2h}^5, No. 14), $a = 9.847(1)$, $b = 7.3418(8)$, $c = 29.563(3)$ Å, $\beta = 92.420(2)°$, $V = 2135$ Å^3. D_c $(Z = 4) = 1.74_8$ g cm^{-3}; $F(000) = 1112$. $\mu_{Mo} = 15.1$ cm^{-1}; specimen: $0.15 \times 0.14 \times 0.12$ mm; $T_{min,max} = 0.73$, 0.88. $N_t = 20549$, $N = 5304$ ($R_{int} = 0.028$), $N_o = 4590$; $R = 0.034$, $R_w = 0.043$. $n_v = 308$, $|\Delta\rho_{max}| = 0.80(4)$ e Å^{-3}.

2.2.1.2. Compound ***3c***. $C_{18}H_{17}ClN_4OPd$. CH_2Cl_2, $M = 532.2$. Monoclinic, space group $P2_1/n$ (C_{2h}^5, No. 14, variant), $a = 9.853(1)$, $b = 15.111(2)$, $c = 13.885(3)$ Å, $\beta = 102.493(2)°$, $V = 2018$ Å^3. D_c $(Z = 4) = 1.75_1$ g cm^{-3}. $F(000) = 1064$. $\mu_{Mo} = 13.4$ cm^{-1}; specimen: $0.20 \times 0.12 \times 0.04$ mm; $T_{min,max} = 0.74$, 0.89. $N_t = 24062$, $N = 5219$ ($R_{int} = 0.061$), $N_o = 3412$; $R = 0.042$, $R_w = 0.041$. $n_v = 253$, $|\Delta\rho_{max}| = 1.1(1)$ e Å^{-3}.

2.3. Synthesis of the ligands

The synthesis of bisimidazole ligands **1a**,**b**,**d**,**f** and methods employed for the synthesis of other related mixed donor ligands will be reported elsewhere.

2.4. General procedure for the preparation of neutral complexes

The complexes were prepared by standard methods [15]. Thus, 1.03 equivalents of the ligand were added to a suspension or solution of $[Pd(Cl)_2(COD)]$ and [Pd(Me)(Cl)(COD)] in CH_2Cl_2 and the reaction mixture was allowed to stir overnight. In the cases where the product precipitated from the reaction mixture (**2b**,**e**, **3a**,**b**,**e**) the suspension was allowed to settle and the solution removed via a syringe. The crude product was washed with CH_2Cl_2 ($3 \times$ ca. 10 ml) followed by hexanes ($3 \times$ ca. 10 ml) and dried under vacuum. In the cases of CH_2Cl_2 soluble products (**3c**,**d**,**f**) the solution was filtered through Celite and the solvent removed in vacuo. The solid was washed with ether or hexanes ($3 \times$ ca. 10 ml) and dried under vacuum. Yields for all complexes were $> 90\%$.

2.4.1. $[Pd(Cl)_2\{(mim)_2CO\}]$ (**2b**)

Compound **2b** was isolated as a light brown solid: Anal. Calc. for $C_9H_{10}N_4OCl_2Pd$: C, 29.41; H, 2.74; N, 15.24. Found: C, 29.58; H, 2.56; N, 14.96%. MS (LSIMS) m/z: 332.7, $[M-Cl]^+$ (100%); ^{1}H-NMR (200 MHz, DMSO): δ 7.88 (s, 1H, Im*H*); 7.34 (s, 1H, Im*H*); 4.05 (s, 3H, N–CH_3). IR (KBr): ν (C=O) 1639 cm^{-1}.

2.4.2. $[Pd(Cl)_2\{(mim)_2C=NPh\}]$ (**2d**)

Compound **2d** was isolated as orange needles from a chloroform solution of **3d**: ^{1}H-NMR (200 MHz, DMSO): δ 7.58 (d, 1H, $^4J_{H-H} = 1.3$ Hz, Im*H*), 7.54 (d, 1H, $^4J_{H-H} = 1.9$ Hz, Im*H*), 7.36 (d, 1H, $^4J_{H-H} = 1.1$ Hz, Im*H*), 7.32 (s(br), 1H, Im*H*), 7.22 (d, 1H, $^4J_{H-H} =$ 1.5 Hz, Im*H*), 7.02 (s(br), 1H, Im*H*), 6.9 (s(br), 1H, Im*H*), 6.86 (d, 1H, $^4J_{H-H} = 1$ Hz, Im*H*), 4.09 (s, 3H, N–CH_3), 2.8 (s, 3H, N–CH_3).

2.4.3. $[Pd(Cl)_2\{(mim)PPh_2\}]$ (**2e**)

Compound **2e** was isolated as a brown–orange solid: Anal. Calc. for $C_{16}H_{15}N_2PCl_2Pd$: C, 43.32; H, 3.41; N, 6.32. Found: C, 43.06; H, 3.44; N, 6.25%. MS (ESI in CH_3CN) m/z: 852.7, $[2MH-Cl]^+$ (100%); 448, $[M-Cl+CH_3CN]^+$ (27%). ^{1}H-NMR (200 MHz, DMSO): δ 7.9–7.2 (m, 10H, Ar*H*), 7.12 (d, 2H, $^3J_{H-H} = 2.28$ Hz, Im*H*), 3.68 (s, 3H, N–CH_3); ^{31}P-NMR (400 MHz, DMSO): δ 89 (s).

2.4.4. $[Pd(Me)(Cl)\{(mim)_2CH_2\}]$ (**3a**)

Compound **3a** was isolated as a white solid: Anal. Calc. for $C_{10}H_{15}N_4ClPd$: C, 36.06; H, 4.53; N, 16.82. Found: C, 36.30; H, 4.37; N, 16.74%. MS (LSIMS) m/z: 317, $[M-CH_3]^+$ (11%); 297, $[M-Cl]^+$ (41%); 282, $[M-CH_3-Cl]^+$ (97%); 177, $[Ligand]^+$ (100%). ^{1}H-NMR (400 MHz, DMSO): δ 7.32 (s, 1H, Im*H*); 7.17 (s, 1H, Im*H*); 7.14 (s, 1H, Im*H*); 6.92 (s, 1H, Im*H*); 3.76 (s, 3H, N–CH_3); 3.70 (s, 3H, N–CH_3); 0.46 (s, 3H, Pd–CH_3).

2.4.5. $[Pd(Me)(Cl)\{(mim)_2CO\}]$ (**3b**)

Compound **3b** was isolated as a yellow solid: Anal. Calc. for $C_{10}H_{13}ON_4ClPd$: C, 34.60; H, 3.77; N, 16.14. Found: C, 34.73; H, 3.71; N, 15.98%. MS (ESI in CH_3CN) m/z: 352, $[M-Cl+CH_3CN]^+$ (100%); 337, $[M-Cl-CH_3+CH_3CN]^+$ (54%). ^{1}H-NMR (200 MHz, DMSO): δ 7.83 (s (br), 1H, Im*H*); 7.75 (s(br), 1H, Im*H*); 7.67 (s(br), 1H, Im*H*); 7.34 (s(br), 1H, Im*H*); 4.05 (s, 3H, N–CH_3); 0.68 (s, 3H, Pd–CH_3). IR (KBr): 1633 cm^{-1}.

2.4.6. $[Pd(Me)(Cl)\{(bmim)_2CO\}]$ (**3c**)

Compound **3c** was isolated as a yellow solid: Anal. Calc. for $C_{18}H_{17}N_4OClPd$: C, 48.34; H, 3.83; N, 12.53. Found: C, 47.99; H, 4.03; N, 11.86%. MS (LSIMS) m/z: 411, $[M-Cl]^+$ (30%); 431, $[M]^+$ (11%); 396, $[M-Cl-CH_3]^+$ (100%); 291, $[Ligand]^+$ (57%). ^{1}H-NMR (200 MHz, $CDCl_3$): δ 8.62 (d(br), 1H, $^2J_{H-H} = 12.5$ Hz, Ar*H*), 8.07 (d(br), 1H, $^2J_{H-H} = 10$ Hz, Ar*H*), 7.6–7.4 (m, 6H, Ar*H*) 4.25 (s, 3H, N–CH_3); 4.23 (s, 3H, N–CH_3); 1.12 (s, 3H, Pd–CH_3). IR (KBr): ν (C=O) = 1662 cm^{-1}. Crystals suitable for X-ray analyses were obtained by slow diffusion of petrol ether (60/80) into a CH_2Cl_2 solution of the complex.

2.4.7. $[Pd(Me)(Cl)\{(mim)_2C{=}NPh_2\}]$ (**3d**)

Compound **3d** was isolated as a yellow solid: Anal. Calc. for $C_{16}H_{18}N_5ClPd$: C, 45.52; H, 4.29; N, 16.59. Found: C, 44.65; H, 4.41; N, 15.86%. MS (LSIMS) m/z: 406, $[M-CH_3]^+$ (8%); 386, $[M-Cl]^+$ (26%); 371, $[M-Cl-CH_3]^+$ (100%); 264, $[Ligand]^+$ (53%). ^{1}H-NMR (200 MHz, $CDCl_3$): δ 7.7–7.15 (m, 5H, Ar*H*) 7.1–6.7 (m, 4H, Im*H*), 4.12 (s (br), 3H, N–CH_3), three isomers (*cis*–*trans*{major}/*cis*–*trans*{minor}/imidazole-imine) 2.87/2.79/2.91 (each: s, 3H, N–CH_3), 1.01/0.89/0.96 (each: s, 3H, Pd–CH_3).

2.4.8. $[Pd(Me)(Cl)\{(mim)PPh_2\}]$ (**3e**)

Compound **3e** was isolated as a green–yellow solid: Anal. Calc. for $C_{17}H_{18}N_2PClPd$: C, 48.25; H, 4.29; N, 6.62. Found: C, 47.42; H, 4.58; N, 6.67%. MS (LSIMS) m/z: 811, $[2MH-Cl]^+$ (100%); 781, $[2MH-Cl-2CH_3]^+$ (24%); 443, $[MH-CH_3+Cl]^+$ (31%); 372, $[M-Cl-CH_3]^+$ (19%). ^{1}H-NMR (200 MHz, DMSO): δ 7.9–7.3 (m, 12H, Ar*H* + Im*H*), two isomers (major/minor) 3.13/2.78 (each: s, 3H, N–CH_3), 0.94/0.85 (each: d, 3H, $^3J_{P-H} = 3.8/4.4$ Hz, Pd–CH_3); ^{31}P-NMR (400 MHz, DMSO): two isomers (major/minor) δ 23.9/16.6 (each: s).

*2.4.9. [Pd(Me)(Cl){(mim)CHCH$_2$PPh$_2$}] (**3f**)*

Compound **3f** was isolated as a white solid: Anal. Calc. for $C_{23}H_{26}N_4PClPd$: C, 51.99; H, 4.93; N, 10.54. Found: C, 51.87; H, 4.71; N, 10.27%. MS (LSIMS) *m/z*: 1027, $[2MH-Cl]^+$ (17%); 495, $[M-Cl]^+$ (100%); 295, $[Ligand-C_6H_5]^+$ (68%). ^{1}H-NMR (400 MHz, $CDCl_3$): δ 7.66 (s(br), 2H, Ar*H*) 7.57 (s(br), 2H, Ar*H*), 7.4 (s(br), 7H, 6 Ar*H* + 1 Im*H*), 6.88 (s(br), 2H, Im*H*) 6.42 (s(br), 1H, Im*H*), 5.46 (m (br), 1H, *CH*), 3.60 (m(br), 1H, *CH$_2$*), 3.28 (s(br), 3H, N–*CH$_3$*), 3.16 (s(br), 3H, N–*CH$_3$*), 2.95 (m(br), 1H, *CH$_2$*), 0.61 (d(br), 3H, $^3J_{P-H} = 3.2$ Hz, Pd–*CH$_3$*); ^{31}P-NMR (400 MHz, CD_2Cl_2) δ 29.4 (s(br)).

2.5. General procedure for the preparation of cationic complexes

The complexes were prepared according to the following general procedure [15]. A solution of $AgBF_4$ (or NaBARF (BARF = $[3,5\text{-}(CF_3)_2C_6H_3]_4B^-$), $NaBPh_4$) in CH_3CN/CH_2Cl_2 was added to a well-stirred solution or suspension of the methyl chloro Pd-complex in the same solvent (except for **4d** which was prepared in CH_3CN only). After 1 h at room temperature (r.t.) the solution was separated from the white precipitate by filtration through Celite and the filtrate was evaporated to dryness. The solid was washed with hexanes (3 × 5 ml) and dried under vacuum. Yields in all reactions were > 90%.

*2.5.1. [Pd(Me)(CH$_3$CN){(mim)$_2$CH$_2$}]BF$_4$ (**4a**)*

Compound **4a** was isolated as a white solid: Anal. Calc. for $C_{12}H_{18}N_5BF_4Pd$: C, 33.87; H, 4.26; N, 16.46. Found: C, 33.88; H, 4.13; N, 16.40%. MS (LSIMS) *m/z*: 338, $[M-BF_4]^+$ (10%); 297, $[M-BF_4-CH_3CN]^+$ (41%); 282, $[M-BF_4-CH_3CN-CH_3]^+$ (49%). ^{1}H-NMR (400 MHz, $CDCl_3$): δ 6.98 (s, 1H, Im*H*), 6.76 (s, 1H, Im*H*), 6.62 (s, 1H, Im*H*) 6.59 (s, 1H, Im*H*), 3.49 (s, 3H, N–*CH$_3$*), 3.44 (s, 3H, N–*CH$_3$*), 2.19 (s, 3H, CH_3CN), 0.61 (s, 3H, Pd–*CH$_3$*). IR (KBr): *v* (C≡N) 2314 cm^{-1}.

*2.5.2. [Pd(Me)(CH$_3$CN){(mim)$_2$CO}]BF$_4$ (**4b/BF$_4$**)*

Compound **4b/BF$_4$** was isolated as a yellow solid: Anal. Calc. for $C_{12}H_{16}ON_5BF_4Pd$: C, 32.79; H, 3.67; N, 15.93. Found: C, 33.12; H, 3.23; N, 15.42%. MS (ESI in MeOH/CH_3CN) *m/z*: 352, $[M-BF_4]^+$ (100%); 337, $[M-BF_4-CH_3]^+$ (77%); 296, $[M-BF_4-CH_3-CH_3CN]^+$ (9%). ^{1}H-NMR (400 MHz, CH_2Cl_2/DMSO): δ 7.63 (d, 1H, Im*Hd*), 7.54 (d, 1H, Im*Ha*), 7.40 (d, 1H, Im*Hc*), 7.54 (d, 1H, Im*Hb*), 3.97 (s, 3H, N–*CH$_3\beta$*), 3.96 (s, 3H, N–*CH$_3\alpha$*), 1.93 (s, 3H, CH_3CN), 0.61 (s, 3H, Pd–*CH$_3$*); IR (KBr) *v* (C=O) 1663 cm^{-1}.

*2.5.3. [Pd(Me)(CH$_3$CN){(mim)$_2$CO}]BARF (**4b/BARF**)*

Compound **4b/BARF** was isolated as a white solid: Anal. Calc. for $C_{44}H_{28}ON_5BF_{24}Pd$: C, 43.46; H, 2.32; N, 5.76. Found: C, 43.80; H, 2.00; N, 5.50%. MS (ESI in CH_3CN) *m/z*: 352, $[M-BF_4]^+$ (51%); 337, $[M-BF4-CH_3]^+$ (100%); 296, $[M-BF_4-CH_3-CH_3CN]^+$ (15%). ^{1}H-NMR (200 MHz, CD_2Cl_2): δ 7.73 (m(br), 8H, *o*-Ar*H*), 7.57 (s(br), 4H, *p*-Ar*H*), 7.3 (d, 1H, $^3J_{H-H} = 1.8$ Hz, Im*H*), 7.27 (d, 2H, $^3J_{H-H} = 1.4$ Hz, Im*H*), 7.14 (s(br), 1H, ImH), 4.09 (s, 6H, N–*CH$_3$*), 2.41 (s, 3H, CH_3CN), 0.98 (s, 3H, Pd–CH_3); IR (KBr) *v*(C=O) 1651 cm^{-1}, *v*(C≡N) 2300 cm^{-1}.

*2.5.4. [Pd(Me)(CH$_3$CN){(mim)$_2$CO}]BARF (**4b/BPh$_4$**)*

Compound **4b/BPh$_4$** was isolated as a light brown solid: Anal. Calc. for $C_{36}H_{36}ON_5BPd$: C, 64.35; H, 5.40; N, 10.42. Found: C, 64.54; H, 4.30; N, 9.61%. ^{1}H-NMR (200 MHz, $CDCl_3$): δ 7.7–6.8 (m, 24H, Ar*H* + Im*H*), 4.13 (s, 3H, N–*CH$_3$*), 4.10 (s, 3H, N–*CH$_3$*), 2.01 (s, 3H, *CH$_3$*CN), 0.98 (s, 3H, Pd–CH_3); IR (KBr) *v*(C=O) 1643 cm^{-1}.

*2.5.5. [Pd(Me)(CH$_3$CN){(bmim)$_2$CO}]BF$_4$ (**4c**)*

Compound **4c** was isolated as a yellow solid: Anal. Calc. for $C_{20}H_{20}ON_5BF_4Pd$: C, 44.52; H, 3.73; N, 12.98. Found: C, 43.76; H, 3.53; N, 12.80%. MS (LSIMS) *m/z*: 452, $[M-BF_4]^+$ (26%); 411, $[M-BF_4-CH_3CN]^+$ (84%); 396, $[M-BF_4-CH_3CN-CH_3]^+$ (100%). ^{1}H-NMR (200 MHz, CD_2Cl_2): δ 7.93 (pseudo triplet, 2H, *o*-Ar*H*), 7.78 (m, 6H, Ar*H*), 4.34 (s, 3H, N–*CH$_3$*), 4.25 (s, 3H, N–*CH$_3$*), 2.31 (s, 3H, *CH$_3$*CN), 1.12 (s, 3H, Pd–*CH$_3$*); IR (KBr) *v* (C=O) 1669 cm^{-1}, *v* (C≡N) 2314 cm^{-1}.

*2.5.6. [Pd(Me)(CH$_3$CN){(mim)$_2$C=NPh}]BF$_4$ (**4d**)*

Compound **4d** was isolated as a yellow solid: Anal. Calc. for $C_{18}H_{21}N_6BF_4Pd$: C, 42.0; H, 4.12; N, 16.33. Found: C, 39.24; H, 4.27; N, 15.04%. MS (LSIMS) *m/z*: 427, $[M-BF_4]^+$ (6%); 386, $[M-BF_4-CH_3CN]^+$ (18%); 371, $[M-BF_4-CH_3CN-CH_3]^+$ (37%). ^{1}H-NMR (200 MHz, CD_2Cl_2): δ 7.7–6.8 (m, 9H, Ar*H*), three isomers (*cis–trans* {major} /*cis–trans* {minor}/imidazole-imine) each: 4.16/4.12/4.08 (s, 3H, N–*CH$_3$*), 2.88/2.84/2.92 (s, 3H, N–*CH$_3$*), 2.42/2.46/2.49 (s, 3H *CH$_3$*CN), 1.0/0.89/0.97 (s, 3H, Pd–*CH$_3$*).

*2.5.7. [Pd(Me)(CH$_3$CN){(mim)PPh$_2$}]BF$_4$ (**4e**)*

Compound **4e** was isolated as a yellow solid: Anal. Calc. for $C_{19}H_{21}N_3PBF_4Pd$: C, 44.26; H, 4.10; N, 8.15. Found: C, 43.79; H, 3.68; N, 8.07%. MS (LSIMS) *m/z*: 943, $[2M-BF_4]^+$ (50%); 811, $[2MH-CH_3-CH_3CN-C_6H_5]^+$ (17%). ^{1}H-NMR (200 MHz, CD_2Cl_2): δ 7.63 (m, 10H, Ar*H*), 7.57 (s, 1H, Im*H*), 7.53 (s, 1H, Im*H*), 4.34 (s, 3H, N–*CH$_3$*), 3.24 (s, 3H, N–*CH$_3$*), 1.77 (s, 3H, *CH$_3$*CN), 1.32 (d, 3H, $^3J_{P-H} = 3.6$ Hz, Pd–*CH$_3$*).

*2.5.8. [Pd(Me){(mim)$_2$CHCH$_2$PPh$_2$}]BF$_4$ (**4f**)*

Compound **4f** was isolated as a white solid: Anal. Calc. for $C_{23}H_{26}N_4PBF_4Pd$: C, 47.4; H, 4.51; N, 9.62. Found: C, 47.22; H, 4.82; N, 9.36%. MS (LSIMS) m/z: 495, $[M-BF_4]^+$ (100%); 295, $[Ligand-C_6H_6]^+$ (56%). ^{1}H-NMR (200 MHz, DMSO): δ 7.7–7.3 (m, 10H, Ar*H*), 7.05 (m, 3H, Im*H*), 6.86 (s, 1H, Im*H*), 4.82 (q(br), $^3J_{H-H} = 12.8$ Hz 1H, *CH*), 3.92 (s, 3H, N–*CH$_3$*), 3.2 (s(br), 5H, *CH$_2$* + N–*CH$_3$*), −0.55 (d, 3H, $^3J_{P-H} = 3.4$ Hz, Pd–*CH$_3$*).

2.6. Variable temperature NMR studies of CO and ethylene insertions into cationic methyl complexes

CD_2Cl_2 was added to a NMR tube charged with the desired complex under a nitrogen atmosphere. For the less soluble complexes d_6-DMSO was added dropwise until complete dissolution was obtained. The tube was closed with a septum fitted with two needles, one reaching into the solution. The tube was immersed into a cooling bath set to the desired temperature and a gentle stream of CO or ethylene was bubbled through the solution for approximately 3 min.

*2.6.1. [Pd(Me)(CH$_3$CN){(mim)$_2$CO}]BARF (**5b**), [Pd(Me)(CO){(mim)$_2$CO}]BARF (**5b′**) (observed in situ (NMR) at −60°C)*

^{1}H-NMR (400 MHz, CD_2Cl_2): δ 7.3, 7.27, 7.24, 7, 7.02, 6.97, 6.90, 6.86 (each: s, 1H, Im*H* (**5b**, **5b′**)), 4.02, 4.01, 3.99, 3.97 (each: s)(6H, N–*CH$_3$*), 2.67 (s, 3H, Pd–C(O)*CH$_3$* (**5b′**)), 2.47 (s, 3H, Pd–C(O)*CH$_3$* (**5b**)), 2.36 (s, 3H, *CH$_3$*–CN (**5b**)).

2.7. Catalytic Heck coupling of n-butyl acrylate and 4-bromoacetophenone

In a typical run, a 100 ml Schlenk flask was charged with 4-bromoacetophenone (4.98 g, 25 mmol) and anhydrous sodium acetate (2.29 g, 27.92 mmol), and degassed by successive vacuum-nitrogen cycles. *N*,*N*-Dimethylacetamide (25 ml) and *n*-butyl acrylate (5 ml, 27.5 mmol) were then added. The complex (2.5×10^{-5} mmol) was dissolved in *N*,*N*-dimethylacetamide (10 ml) and 0.1 ml of this solution injected into the reaction mixture which was then heated to 120°C. After 24 h the mixture was allowed to cool and di(ethylene glycol)butyl ether (500 μl) added. A sample of the solution (500 μl) was taken, injected into a sample vial containing 5% HCl (5 ml) and extracted with 2.5 ml of CH_2Cl_2. The CH_2Cl_2 extracts were analysed by gas chromatography.

2.8. Catalytic copolymerisation of CO and ethylene

Catalytic copolymerisation of CO and ethylene was carried out in a 75 ml stainless steal test autoclave which was dried at 100°C and cooled to r.t. under vacuum.

2.8.1. General procedure

A solution of the complex in CH_2Cl_2 (40 ml) was transferred into the autoclave under nitrogen. The autoclave was weighed then charged with 20 bar of ethylene followed by 20 bar of carbon monoxide at r.t. The vessel was then placed into an oil bath at 90°C and allowed to equilibrate at 50°C, at which point timing was started. The mixture was stirred for 1 h at 50°C then cooled to r.t. in an ice bath. The pressure was slowly released and the autoclave reweighed. The reaction mixture was filtered and the filtrate analysed by GC. The solid was washed with CH_2Cl_2 and dried in air. Values typically found for the grey–white solids: Anal. Calc. for C_3H_4O: C, 64.26; H, 7.21. Found: C, 63.14; H, 7.38%. IR (KBr): ν(C=O) 1694 cm^{-1}.

3. Results and discussion

3.1. Preparation and characterisation of neutral and cationic complexes

The imidazole chelate ligands **1a** and **1b** [11,12a] (Fig. 1) have been synthesised by modified literature procedures. Thus, lithiation of *N*-methylimidazole and subsequent reaction with diethylcarbonate at low temperature in THF afforded the keto bridged **1b**. The methylene bridged bis-imidazole **1a** was obtained by Wolff–Kishner reduction of **1b**. These compounds served as precursors for the new ligands **1d** and **1f**. Treatment of a CH_2Cl_2 solution of **1b** with a slight excess of aniline in the presence of $TiCl_4$ gave the imine derivative **1d**. Deprotonation at the bridging methylene group in **1a** with BuLi followed by reaction with Ph_2CH_2Cl [18] at low temperature in THF afforded **1f**. A paper describing synthetic details for these and other related ligands will be published elsewhere. Compound **1c** was prepared as previously reported [16] and **1e** following a procedure given for the *N*-benzyl derivative [17].

Reaction of [PdCl$_2$(COD)] or [PdMeCl(COD)] with 1.05 equivalents of the respective ligand in CH_2Cl_2 afforded the neutral dichloro and chloro, methyl complexes in yields >90% (Scheme 1). Generally the methyl, chloro complexes appear to be lighter in colour than their dichloro counterparts. Complexes **2b–d** and **3a–c** are relatively air and temperature stable compounds, whereas **2e**, **3e**,**f** are air sensitive due to facile oxidation of the phosphorus. In chloroform solution the imine complex **3d** undergoes elimination of the methyl group, even at r.t. Within 1 or 2 days orange needles, which were identified by crystal structure determination (see below) as the respective dichloro complex

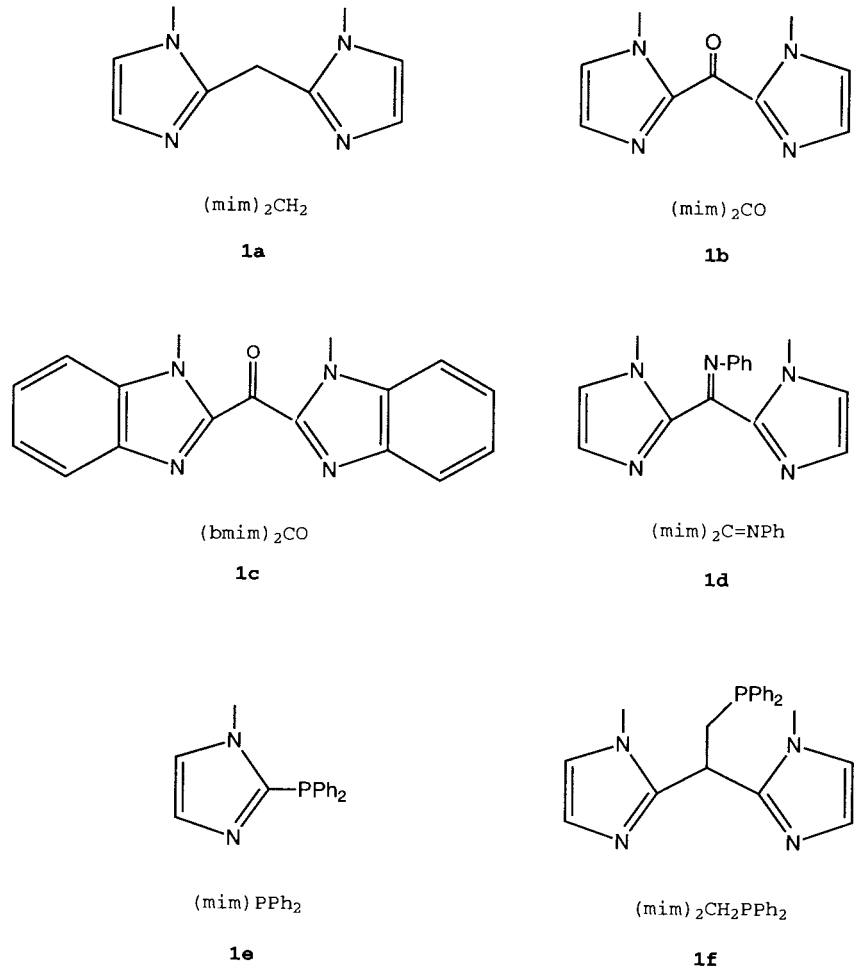

Fig. 1. 1,1-Methylimidazole based chelate ligands used in the preparation of palladium complexes.

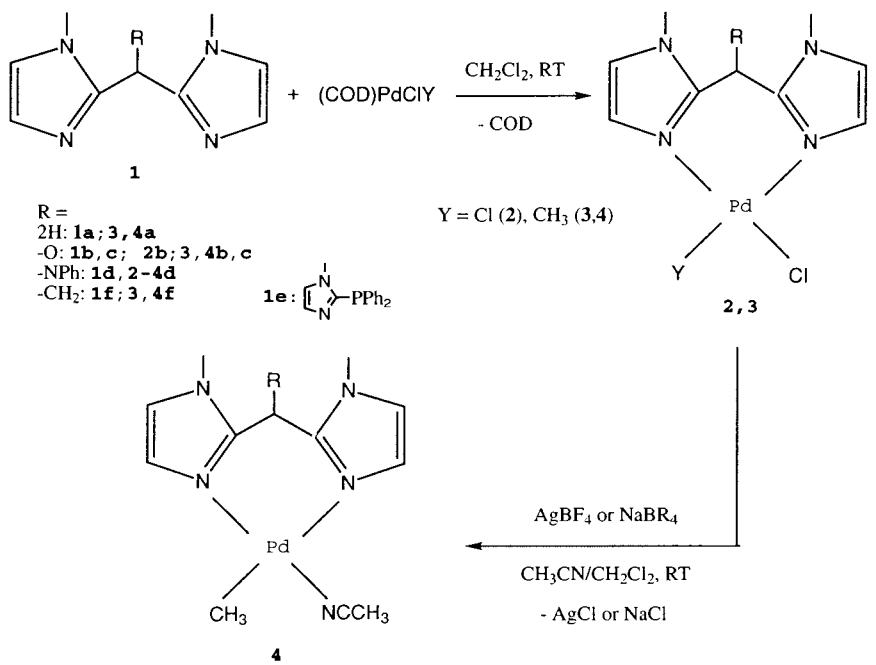

Scheme 1.

Table 1
Selected ^{1}H-NMR data for neutral complexes

Complex	Solvent	Pd–CH_3	N–CH_3
2b	DMSO	–	4.05
2d	DMSO/$CDCl_3$	–	2.79/4.09
2e	DMSO	–	3.68
3a	DMSO	0.46	3.70/3.76
3b	DMSO	0.68	4.05
3c	$CDCl_3$	1.12	4.23/4.25
3d [a]			
	$CDCl_3$		
	1.01, 0.89, 0.96	2.87/4.12 (br), 2.79/4.12 (br), 2.91/4.12 (br)	
3e [b]	DMSO	0.85/0.94	2.78/3.13
3f	$CDCl_3$	0.61	3.16/3.28

[a] Three isomers.
[b] Two isomers.

Table 2
Selected ^{1}H-NMR data for cationic complexes

Complex	Solvent	Pd–CH_3	N–CH_3	NC–CH_3
4a	$CDCl_3$	0.31	3.44/3.49	2.19
4b/BF_4	DMSO	0.76	4.04	–
4b/BF_4	CD_2Cl_2/DMSO	0.0/0.73	4.06	2.05/(1.94)
4b/BARF	CD_2Cl_2	0.98	4.09	2.41
4c	CD_2Cl_2	1.12	4.25/4.34	2.31
4c	CD_2Cl_2/DMSO	0.79/0.94	4.11	2.26/(1.99)
4d [a]	CD_2Cl_2	1.0, 0.89, 0.97	2.88/4.16, 2.84/4.12, 2.92/4.08	2.42, 2.46, 2.49
4e	CD_2Cl_2	1.31	3.24	1.77
4f	DMSO	−0.55	3.2/3.92	–

[a] Three isomers.

2d, crystallised from the $CDCl_3$ solution. Complexes **2d**, **3c**,**d**,**f** are soluble in CH_2Cl_2 and $CHCl_3$ whereas **2b**, **3a**,**b** require DMSO as a solvent. Complexes **2e** and **3e** are only sparingly soluble in DMSO.

The cationic acetonitrile complexes **4a**–**e** were prepared in $>90\%$ yields from the respective chloro complexes in CH_3CN or CH_3CN/CH_2Cl_2 solution by halide abstraction with silver or sodium salts (Scheme 1). The complex **4f** contains no ancillary solvent ligand and hence the remaining coordination site is occupied by the third donor function of the ligand **1f** (see discussion below). The cationic complexes are unstable in solution over extended periods at r.t. Decomposition in solution was significantly more rapid for **4d** and precipitation of a brown black solid from CH_2Cl_2 solutions occurred within a few minutes. The cationic complexes **4b/BARF** ($BARF = [3,5\text{-}(CF_3)_2C_6H_3]_4B^-$) [19] and **4b/$BPh_4$** were prepared by treatment with the sodium salts of the anions. Stabilities were found to decrease in the order $BF_4^- > BARF^- > BPh_4^-$. A similar trend in stabilities was observed by Macchioni et al. [18] who investigated the counterion effect on the ethylene/CO copolymerisation for cationic Pd(II) bipy complexes. The compounds can be kept over weeks without decomposition when stored as solids at −20°C.

Full characterisation of the complexes was accomplished by ^{1}H-NMR, MS, IR, and microanalysis. Selected ^{1}H-NMR data are shown in Table 1 (neutral complexes) and Table 2 (cationic complexes).

A downfield shift of the Pd–CH_3 resonance is observed for the complexes **3b**–**d** and **4b**–**d** compared to **3a** and **4a** which reflects the influence of the electron withdrawing C=O and C=N–Ph groups present in the ligand backbone, on the metal centre.

Mass spectra analysis of the imidazole phosphine complexes **2e**, **3e** and **4e** provided evidence for the expected dimeric structures. For an analogous ligand, diphenylphosphine(1-benzylimidazol-2yl), a dimeric gold complex was reported [17], and the related pyridine ligand has been shown to act as a bridging ligand in Rh and Pd complexes [21]. The ^{1}H- and ^{31}P-NMR spectra of **2e** display one singlet for the CH_3–N group ($\delta = 3.68$ ppm) and for phosphorus ($\delta = 89$ ppm), respectively, indicating the presence of one isomer, the exact structure of which is uncertain (whether head-to-tail or head-to-head; Fig. 2). For **3e** evidence for the formation of two of the four possible isomers (Fig. 2) was detected. The ^{31}P-NMR spectrum displays singlets at $\delta = 23.9$ and 16.6 ppm. The Pd methyl resonances of **3e** ($\delta = 0.94$ ppm, $^3J_{P-H} = 3.8$ Hz, and 0.85 ppm,

$^3J_{P-H} = 4.3$ Hz) appear as doublets with coupling constants indicating *cis* arrangements for the phosphorus and methyl group. Similar values were found by Vrieze et al. [22] for Pd and Pt complexes with P–N ligands.

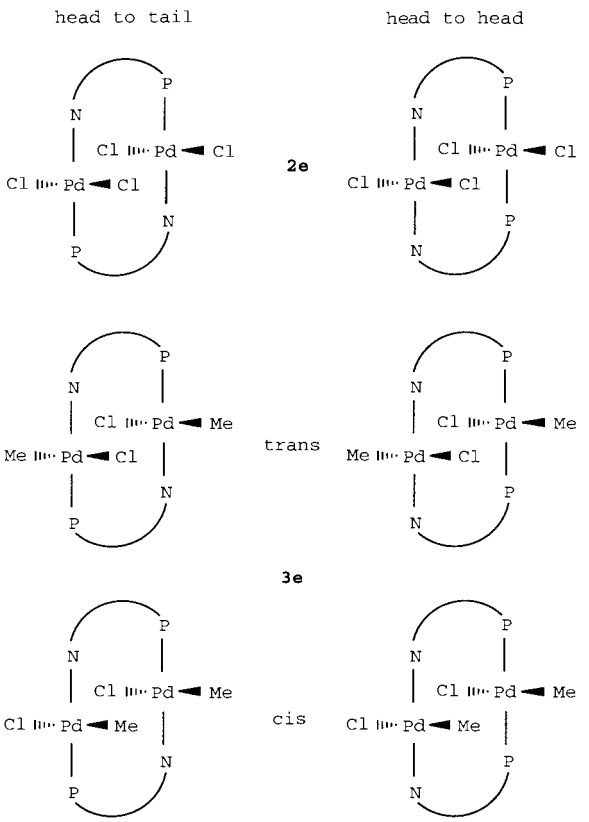

Fig. 2. Possible 'head-to-tail' and 'head-to-head' isomers of **2e** and **3e**.

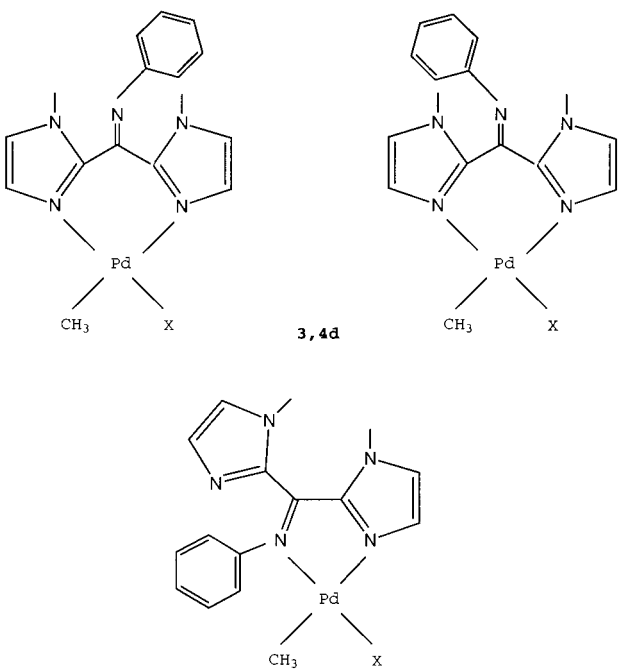

Fig. 3. Isomers of **3d** and **4d.**

Since both Pd–CH_3 resonances appear as doublets the possibility of the second isomer being the head-to-head isomer can be excluded and therefore the formation of head-to-tail isomers with the methyl groups either *trans* or *cis* to each other is very likely. For the complex **4e**, one singlet at 17.4 ppm in the ^{31}P-NMR spectrum and one doublet at 1.32 ppm ($^3J_{P-H} = 3.8$ Hz) in the ^{1}H-NMR spectrum indicate the presence of one isomer only.

The imino function in the ligand backbone of **3d** gives rise to two sets of signals in the ^{1}H-NMR spectrum due to the formation of the two possible isomers (Fig. 3) in a ratio of approximately 1.7:1. A third set of signals of low intensity, with similar shift values, presumably belongs to a third isomer in which the ligand is coordinated via one imidazole ring and the imino function. The ^{1}H-NMR spectrum of **4d** exhibits the expected sets of resonances for the three possible isomers of **4d** (Table 2). In addition a singlet for free CH_3CN and other signals belonging to unidentified decomposition products are present owing to the limited stability of **4d**.

Complexes **3f** and **4f** are particular interesting since they contain the new tridentate mixed donor ligand **1f**. A doublet for the Pd–CH_3 group in **3f** at $\delta = 0.61$ ppm ($^3J_{P-H} = 3.2$ Hz) reveals N–P coordination in which the soft Pd centre prefers the soft P donor. All signals are broad at r.t. indicating a slow dynamic process, which involves exchange between coordinated and uncoordinated groups. Canty et al. has reported similar fluxional behaviour for the symmetrical and unsymmetrical tridentate ligands [$(pz)_2$(mim)CH], [$(pz)_2$(py)CH], [$(py)_2$(mim)CH] and [(py)$(mim)_2$CH] when coordinated to $PdMe_2$ and PdMeI fragments [12b].

Surprisingly, no coordinated CH_3CN could be detected in the NMR spectrum of **4f** after removal of the solvent under reduced pressure and microanalysis confirmed the absence of the solvent ligand. The compound was only soluble in hot DMSO but remained in solution on cooling to r.t. No signs of decomposition were observed. Removal of the solvent under reduced pressure and a second addition of DMSO led to the same observation. The ^{1}H-NMR (d_6-DMSO) of **4f** shows bidentate coordination by two of the three donor atoms and coordination by DMSO. The appearance of a doublet for the Pd–CH_3 group ($\delta = -0.55$ ppm, $^3J_{P-H} = 3.4$ Hz) and two singlets for the CH_3–N group ($\delta = 3.19$ and 3.92 ppm) indicate P–N coordination of the ligand. The coordination of the σ-donor DMSO gives rise to a large upfield shift of the Pd–CH_3 group compared to **3f**. It is apparent that the ligand in **4f** displays hemilabile behaviour with one imidazole ring dangling in the presence of coordinating solvents and becoming coordinating when the solvent is removed. We therefore conclude that coordination of all three

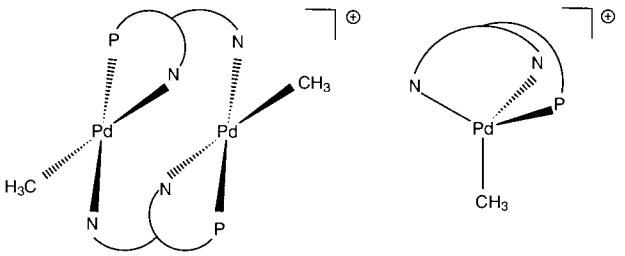

Fig. 4. Possible structures for **4f**.

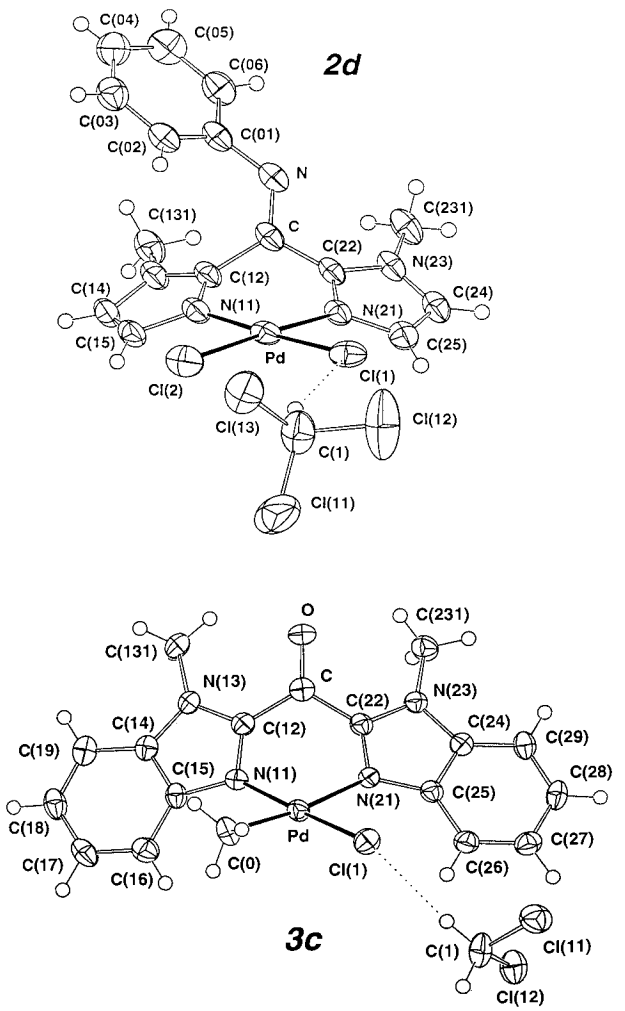

Fig. 5. Projection of **2d** and **3c** with their associated solvent molecules. Fifty percent displacement ellipsoids are shown for ther non-hydrogen atoms having arbitrary radii of 0.1 Å.

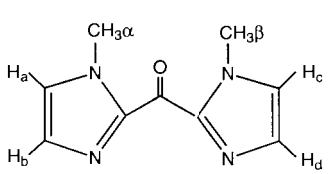

Fig. 6. Annotation of protons of (mim)2CO in **4b**, assigned by COSY NMR experiments.

donors occurs in solid, desolvated **4f.** Although there is no evidence for the presence of a dimeric species in the mass spectrum of **4f** ([M] = 495 (100%)), we are unable to unambiguously decide whether the complex adopts a dimeric structure in which **1f** acts as a bridging ligand or whether it has a monomeric structure with a trigonal pyramidal geometry around the Pd centre (Fig. 4). The insolubility of **4f** in common non-coordinating solvents prevented the growth of crystals. Vrieze et al. [3c,15] reported cationic PdMe complexes bearing tridentate nitrogen ligands, which coordinate via all three donor atoms. Because of the flexibility of the ligands Pd adopts a square planar geometry in these complexes. Interestingly, for the related neutral PdMeCl complexes they observed that only one of the ligands, containing a imidazole ring, has a strong tendency to coordinate in a tridentate fashion whereas the other closely related ligands prefer bidentate coordination [3c].

*3.2. Crystal structures of the complexes [$PdCl_2${$(mim)_2NPh$}] (**2d**) and [PdMeCl{$bmim)_2CO$}] (**3c**)*

Complexes **2d** and **3c** were characterised by X–ray crystallography (Fig. 5). Selected bond distances and angles are given in Table 3. The results of the low-temperature single-crystal X-ray structure determinations are in accord with the stoichiometries, connectivities and stereochemistries proposed/implied above. In each case, a single molecule of complex, accompanied by a single molecule of hydrogen-bonded solvent—chloroform and dichloromethane, respectively, comprise the asymmetric unit of the structure.

The palladium atoms, as might be expected, are found in the common, four-coordinate 'square-planar' environment, comprising a pair of essentially equivalent chelating Pd–N (bidentate) interactions, opposed by a pair of unidentate *trans* interactions. However, in complex **3c** containing the 'fused' benzimidazole ligand the narrow bite angle [N(11)–Pd–N(21) = 85.6(1)°] causes distortion of the square planar structure. In comparison the bite angle in **2d** [N(11)–Pd–N(21) = 88.5(1)°] deviates only slightly from the ideal value. A similar observation was made by Jordan et al. for the bispyrazolyl complexes [$PdCl_2${$Ph_2C(3$-^{t}Bu-$pz)_2$}] [83.62(8)°] and [$PdCl_2${$Ph_2C(pz)_2$}] [89.51(8)°] [7] and Canty et al. reported similar bite angles for tris pyrazolata Pd(IV) complexes [23].

One Pd–Cl interaction is common to both **2d** and **3c**; Pd–Cl(1) differ appreciably, longer in **3c** by ca. 0.03 Å, in keeping with the considerable diminution in bidentate ligand bite, presumably consequent on substitution of CNPh in **2d** by CO in **3c**. The Pd–N interaction, Pd–N(21), reflects the differing *trans*-effects of methyl versus Cl(2), an effect which presumably also correlates with the change in bite of the bidentate ligand, and also

in the *cis* N–Pd–X angles, which, symmetrical in **2d**, become appreciably different in **3c**. The Pd–N(21) bond [2.156(3) Å] *trans* to the methyl group in **3c** is significantly longer than the Pd–N(11) bond [2.042(3) Å] *trans* to the chloride group which is in keeping with the greater *trans* effect of the methyl group and similar values have been reported for other nitrogen chelate Pd complexes [3a,d,i,24].

While N(coordinated)–C distances are identical between the two compounds, it is of interest to observe the significant differences in Pd–N–C(2,5) angles, consequent upon the change in coordinating entity from a simple imidazole to a benzimidazole (Table 3). Other angular parameters of the C_3N_2 array remain similar for the two complexes, except insofar as the arrays are bound together by CO or CNPh, where significant differences, again perhaps attributable to benzimidazole fusion, are found in C–C(*n*2)–N(*n*3).

At the fusion of the two rings, the N,O:CC_2 arrays are effectively planar. Dihedral angles between

Table 3
Selected molecular geometries (**2d**, **3c**) [a]

Atoms	Parameter	Atoms	Parameter
Distances (Å)			
Pd–Cl(1)	2.2916(8), *2.323(1)*	Pd–Cl(2)/C(0)	2.2964(9), *2.030(4)*
Pd–N(11)	2.020(3), *2.042(3)*	Pd–N(21)	2.031(2), *2.156(3)*
N(11)–C(12)	1.331(4), *1.338(5)*	N(21)–C(22)	1.324(1), *1.323(5)*
N(11)–C(15)	1.385(4), *1.389(5)*	N(21)–C(25)	1.372(4), *1.374(5)*
C(12)–N(13)	1.359(4), *1.364(5)*	C(22)–N(23)	1.353(3), *1.367(5)*
N(13)–C(14)	1.376(4), *1.378(5)*	N(23)–C(24)	1.361(4), *1.374(5)*
C(14)–C(15)	1.341(5), *1.393(6)*	C(24)–C(25)	1.363(5), *1.414(5)*
C(12)–C	1.481(4), *1.489(6)*	C(22)–C	1.461(4), *1.489(6)*
C–N/O	1.284(4), *1.212(5)*	Cl(1)···C(1)	3.374(4), *3.597(5)*
H(1)···Cl(1)	2.48(3), *2.66(est.)*		
Angles (°)			
N(11)–Pd–N(21)	88.5(1), *85.6(1)*	Cl(1)–Pd–Cl(2)/C(0)	90.57(3), *87.9(1)*
N(11)–Pd–Cl(2)/C(0)	91.03(7), *90.6(1)*	N(21)–Pd–Cl(1)	89.95(7), *95.65(9)*
N(11)–Pd–Cl(1)	177.50(7), *176.8(1)*	N(21)–Pd–Cl(2)/C(0)	176.93(6), *173.2(2)*
Pd–N(11)–C(12)	124.0(2), *119.6(3)*	Pd–N(21)–C(22)	125.6(2), *119.3(3)*
Pd–N(11)–C(15)	129.5(2), *131.1(3)*	Pd–N(21)–C(25)	126.9(2), *132.6(2)*
C(12)–N(11)–C(15)	106.0(3), *105.7(3)*	C(22)–N(21)–C(25)	107.4(2), *105.7(3)*
N(11)–C(12)–C	124.1(3), *125.3(4)*	N(21)–C(22)–C	123.2(2), *124.9(4)*
N(11)–C(12)–N(13)	110.5(2), *111.9(3)*	N(21)–C(22)–N(23)	109.9(3), *112.7(4)*
C–C(12)–N(13)	125.4(3), *122.7(3)*	C–C(22)–N(23)	126.9(3), *122.3(3)*
C(12)–N(13)–C(14)	106.7(3), *106.7(3)*	C(22)–N(23)–C(24)	107.4(2), *106.6(3)*
N(13)–C(14)–C(15)	107.5(3), *130.7(4)*	N(23)–C(24)–C(25)	107.4(3), *135.9(4)*
C(14)–C(15)–N(11)	109.2(3), *108.8(4)*	C(24)–C(25)–N(21)	107.9(3), *109.1(3)*
C(12)–C–C(22)	114.5(2), *117.5(4)*	C–N–C(01)	123.0(2), –
C(12)–C–N/O	126.7(3), *121.4(4)*	C(22)–C–N/O	118.7(2), *121.0(4)*
Cl(1)···H(1)–C(1)	152(3), *163(est.)*		
Plane parameters (deviations δ (Å); dihedrals θ (°))			
(a) The $N_2Cl(1)Cl(2)/C(0)$ array (χ^2 1340, 134)			
δN(11)	0.085(3), *0.027(4)*	δN(21)	−0.073(3), *−0.023(4)*
δCl(1)	0.010(1), *0.003(1)*	δCl(2)/C(0)	−0.010(1), *−0.043(5)*
δPd	0.014(1), *0.071(2)*	θ/O,NC_3	57.69(8), *61.3(1)*
θ/im(1)	22.4(1), *45.6(1)*	θ/im(2)	28.5(1), *39.7(1)*
(b) The (benz)imidazole C_3N_2/C_7N_2 planes			
χ^2(1)	22, *159*	χ^2(2)	13, 32
θ_1/O,NC_3	49.1(1), *24.3(2)*	θ_2/O,NC_3	39.3(1), *25.9(1)*
θ(1/2)	39.0(1), *28.9(1)*		
δPd_1	0.247(5), *0.647(5)*	δPd_2	0.137(5), *0.517(5)*
δC_1	0.100(6), *0.153(6)*	δC_2	−0.003(5), *0.054(6)*
(c) The central ring N(11,21)C(12,22) plane (χ^2 387, 92)			
θ/im(1)	22.5(1), *15.6(1)*	θ/im(2)	16.9(1), *13.3(1)*
δPd	0.509(4), *0.955(5)*	δC	0.442(4), *0.289(6)*
		δN/O	1.195(6), *0.690(8)*

[a] The two values in each entry are for **2d, 3c**, respectively, the latter *italicized*. In **2d**, the dihedral angle between the phenyl C_6 plane and the NC_3 plane is 42.1(1)°; it is also at 39.8(1)° to the coordination plane and 51.8(1), 12.9(1)° to the C_3N_2(im) planes.

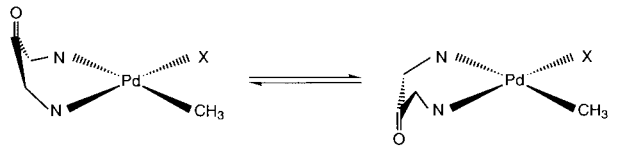

Fig. 7. Fluxional boat-to-boat inversion of the chelate ring in **4b**.

N,O:CC_2 and the co-ordination planes differ by only a few degrees (Table 3). Significant differences are found between the pitches of the individual planes within each complex (taking for example the co-ordination plane as the reference in each case), of ca. 6°, with even greater differences between the pitches of counterpart planes of the two complexes. Those for **3c** are much more steeply inclined than those for **2d**, relative to the co-ordination plane, with the consequence that C(0) deviates much more from the coordination plane in **3c** than C(N) in **2d**. It may be that in **3c**, contacts between the methyl ligand and the neighbouring benzimidazole group influence moiety dispositions. The resultant chelate rings, $Pd(NC)_2C$, formed by the ligands, may be described in terms of a 'boat' conformation. Taking the $(NC)_2$ array as a datum'plane' in each case, the palladium atom deviates by appreciably more in **3c** than **2d**; by contrast, the deviation of the bridging carbon is less in **3c**, cf. **2d**, both deviations being to the same side of the plane. Similar six-membered boat conformations have been reported for the related bis pyrazolyl complexes [Pd $Cl_2\{(R\text{-}pz)_2CPh_2\}$], R = 3-H, 3-^{t}Bu [7] and [Pd $Cl_2\{(pz)_2CMe_2\}$] [25] in which chelate ligands bond via heterocyclic donors. Analogous structural features had also been described earlier by Canty et al. for related bisimidazole and mixed imidazole/heterocyclic Pd(II) complexes on the basis of variable temperature NMR experiments [12a]. Specific bonding parameters about the metal in the present array are comparable with those established in various other systems. The Pd–CH_3 distance is similar to those found for other sp^3 carbons in bipy and phen ligated Pd(II) complexes [3b,d,i,18,24] but slightly elongated compared to a Pd(II) complex bearing a pyridine-imine chelate ligand [2.01(1) Å] reported by Vrieze et al. [3f].

3.3. Variable temperature NMR studies

Variable temperature NMR studies were carried out on the cationic complexes **4b** $\mathbf{BF_4}$/**BARF** and **4c**/$\mathbf{BF_4}$ to investigate fluxional processes in the complexes. Variable temperature NMR was also used to study insertion of CO/ethylene into the Pd alkyl bond.

Fluxional boat-to-boat inversion for the chelate ring and exchange of the weakly coordinated CH_3CN are observed in **4b**. The ^{1}H-NMR spectrum of **4b**/$\mathbf{BF_4}$, dissolved in CD_2Cl_2/d_6-DMSO at −60°C exhibits two singlets for the N–CH_3 group and four resolved doublets ($^3J_{C-H} = 1.6$ Hz) for the two inequivalent imidazole rings. COSY-NMR experiments at −50°C revealed two independent sets of coupled imidazole olefin peaks ($^3J_{H-H} = 1.2$ Hz). One at low field (7.63 and 7.40 ppm) and the other at 7.54 and 7.17 ppm. The coupling constants are small even for a cis configuration, in fact they are in the order of $^4J_{H-H}$ long range couplings between the N–CH_3 groups and Ha and Hc in the ring (numbering scheme Fig. 6). Long range COSY experiments revealed that the low field imidazole coupled olefins are associated with the higher field N–CH_3 (3.96 ppm $CH_3\alpha$). Ha was therefore assigned the resonance at 7.54 ppm and Hb at 7.17 ppm. Hc has a resonance at 7.40 ppm while Hd is downfield at 7.63 ppm and $CH_3\beta$ at 3.97 ppm. The significant difference in the chemical shift of Hb (at highest field) and Hd (lowest field) reflects their proximity to the asymmetric Pd centre.

Signals for uncoordinated ($\delta = 1.93$ ppm) and coordinated ($\delta = 2.04$ ppm) CH_3CN in a ca. 2.5:1 ratio indicate partial exchange of coordinated CH_3CN for DMSO. The spectrum displays two singlets (0.7 and 0.0 ppm) for the Pd–CH_3 protons. The imidazole signals broaden on warming to −10°C. Between 0 and 10°C the signal for the N–CH_3 protons sharpens whereas the signals for the olefinic imidazole ring protons have almost vanished and the ratio of uncoordinated to coordinated CH_3CN is significantly lowered to ca. 1.3:1. Warming to 30°C gives rise to one broad signal in the olefinic region and a sharp singlet for the N-CH_3 protons. The ratio of uncoordinated to coordinated CH_3CN diminishes to 0.4:1. The disappearance of the olefinic signals between 0 and 10°C, their broadening at 30°C and the changing ratio of uncoordinated to coordinated CH_3CN can be explained by a slow exchange process between CH_3CN and DMSO. Similarly, addition of d_6-DMSO to a solution of **4b**/**BARF** in CD_2Cl_2 (at r.t.) resulted in an upfield shift (0.4 ppm) of the CH_3CN signal and caused the three doublets of the olefinic protons to merge into a broad singlet, indicating exchange of CH_3CN for DMSO.

The four doublets and two singlets observed for **4b** at −60°C and their broadening at −10°C can be ascribed to a fluxional process involving the slow inversion of the chelate ring (Fig. 7) which adopts a boat conformation in the solid state as shown by the crystal structures of **2d** and **3c**. Similar behaviour was observed for the related complexes [$PdCl_2\{(pz)_2CMe_2\}$] [25], [PdMeX$\{(pz)_2CHR\}$] [PdMeX$\{(py)_2CHR\}$] (R = H, Me; X = Me, I) [12a] and more recently [$PdCl_2$-$\{(pz)_2Ph_2C\}$] [7]. The slower ring inversion in **4b** compared to the methylene bridged [PdMeI$\{(mim)_2CH_2\}$] [12a] which gives a singlet for the methylene protons down to −70°C may be ascribed to a more rigid bridge containing sp^2 hybridised carbon. We cannot completely rule out a donor induced dissociative exchange

process (presence of DMSO) for **4b/BF$_4$**, which has also been proposed [20]. However, the broadened resonances of **4b/BARF** observed at r.t. in pure CD_2Cl_2, were completely resolved at −80°C. Similarly, in complex **4c** exchange of CH_3CN for DMSO is observed above 0°C, however boat-to-boat inversion of the chelate ring was not observed. The r.t. ^{1}H-NMR spectrum (CD_2Cl_2) shows two singlets for the N–CH_3 groups. Down to −60°C (CD_2Cl_2/DMSO) only one set of signals is observed for the *ortho* (doublet) and *meta* (triplet) protons of the benzimidazole ring. Presumably the sterically more demanding benzimidazole rings retard ring inversion in **4c**. A similar observation was made for [$PdCl_2${(R^3-pz)$_2$$Ph_2$C}] (R = H, ^{t}Bu) [7].

3.4. CO insertion studies

In a study of the reaction of **4b/BARF** with CO, at −90°C the ^{1}H-NMR spectrum exhibits signals for unreacted **4b/BARF**, displaced CH_3CN ($\delta = 1.97$ ppm), and three other species. These species are two insertion products **5b** and **5b′**, which are present as the CH_3CN ($\delta = 2.35$ ppm) and CO adducts (Scheme 2), and a species believed to be a palladium methyl, carbonyl complex, which has a singlet at 1.07 ppm downfield from the Pd–CH_3 resonance. Consistent with our proposals van Asselt et al. have reported the formation of two Pd–acyl complexes in the reaction of cationic [Pd(Me)(CH_3CN)(*p*-An-BIAN)]$^+$ with carbon monoxide [3a], and Brookhart et al. have reported the isolation and characterisation of a related methyl, carbonyl complex [Pd(Me)(CO)(phen)]$^+$ along with the respective insertion product [Pd{C(O)Me}(CO)(phen)]$^+$ in a carbonylation reaction at −78°C [3c,5b]. The signal at 1.07 ppm disappears on warming to −70°C, and no signal for coordinated CH_3CN in this species could be detected. These observations, the presence of uncoordinated CH_3CN, and the weak coordination of CH_3CN, reflected in the formation of two insertion products **5b** and **5b′**, support a dissociative mechanism for the carbonylation of **4b**, i.e. insertion occurring from a four-coordinated intermediate [5b,c,20,26]. However, a carbonylation pathway which occurs from a five-coordinated intermediate [3g,18,27] cannot be completely ruled out.

Insertion of CO into the Pd–CH_3 bond in **4b** is complete at −60°C. The shift values for the acyl methyl group ($\delta = 2.67$ (CO adduct) and 2.47 ppm (CH_3CN adduct) are similar to those reported for other Pd–acyl complexes containing chelating nitrogen ligands [3a–c,e,j]. The CH_3CN signals broaden at −20°C and almost disappear at 0°C indicating a slow exchange of free and coordinated CH_3CN at this temperature. Warming to r.t. causes broadening of both acyl singlets accompanied by coalescence of the CH_3CN signals.

By contrast, carbonylation of the benzimidazole complex **4c** required higher temperatures. Insertion of CO was complete only above −10°C (CH_3(O)C–Pd: $\delta = 2.39$ ppm). Presumably steric crowding caused by the benzimidazole rings retards the CO insertion [3a].

3.5. Ethylene insertion studies

Ethylene insertion into the Pd–acyl bond has been studied for **5b** but the formation of various intermediates which occur in this reaction [3c] and the presence of CH_3CN leading to exchange processes hampers the unambiguous assignment of the observed signals. However, at −90°C the two acyl signals, the N–CH_3 resonance and the signal for coordinated CH_3CN for **5b** and **5b′** are broad indicating a slow exchange process. Coalescence is observed at −60°C giving rise to new broadened resonances for Pd–C(O)CH_3 ($\delta = 2.53$ ppm) and N–CH_3 ($\delta = 4$ ppm) which can be ascribed to the formation of the expected ethylene, acyl complex [Pd{C(O)Me}(C_2H_4){($mim)_2$CO}]$^+$. Consistent with ethylene CH_3CN exchange a broad signal is observed for CH_3CN at 2.0 ppm. Due to the formation of

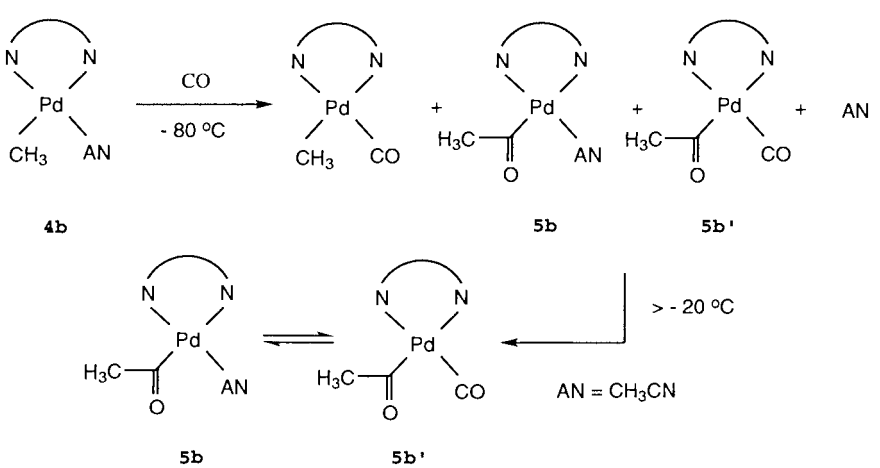

Scheme 2.

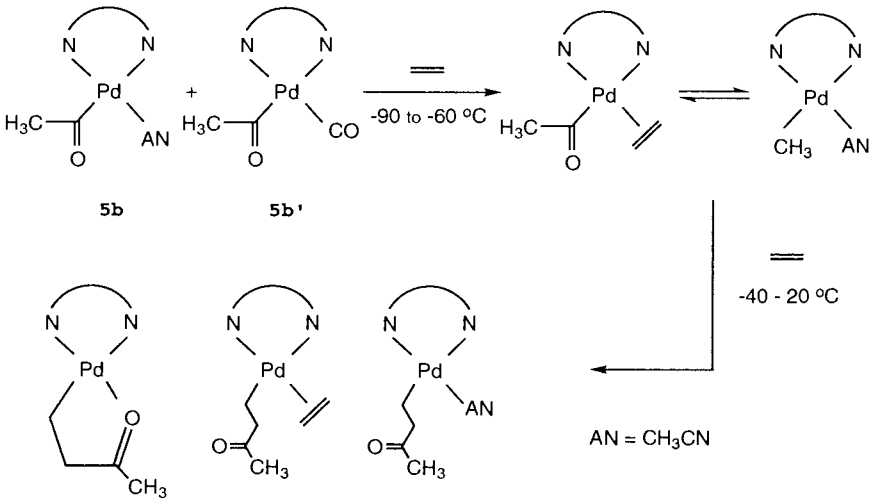

Scheme 3.

various intermediates a series of new signals appears between −40 and +20°C. The presence of expected triplets between 3.1 and 2 ppm provides clear evidence for the formation of insertion products in which either carbon monoxide, ethylene and/or CH_3CN occupy the fourth coordination side (Scheme 3).

3.6. Catalysis

The results obtained from catalytic experiments (Tables 4 and 5) with these new imidazole based Pd complexes provides information on ligand influences and hence the catalytic behaviour of the respective complexes.

Heck coupling reactions [28,29] were carried out using bromoacetophenone/*n*-butylacrylate as a test system. TONs of up to 5 750 000 and 1 700 000 have been reported in this reaction for phosphine palladacycles [29b] and palladium complexes of chelating carbene based ligands [29e] respectively. Reports on Heck-coupling reactions, involving nitrogen-ligated complexes are scarce [30]. For the keto bridged bisimidazole complex **3b** (entry 2, Table 4) high turnover numbers, comparable to those reported for monodentate carbene complexes [PdMe(carbene)(β-diketone)] [29c] were obtained. In comparison, **3c** is about half as active as **3b**, whereas **3a** shows very little activity at all and gives unidentified brominated products.

A similar behaviour is observed when the complexes were tested for ethylene/CO copolymerisation (Table 5). Only **4b** (entries 2–4, 6) catalysed the production of polyketone. Activities however are low compared to those reported for bisphosphine coordinated palladium complexes (10^6 mol C_2H_4/mol Pd) [5d,e]. Catalysis is accompanied by decomposition (grey polymer from Pd deposition). The catalytic performance reflects the expected dependence on the counterion employed (entries 2, 5, 6). Early catalyst decomposition might be the reason for the inactivity of **4d** which appeared to be unstable in chlorinated solvents. Surprisingly complex **4f** containing the tridentate ligand **1f** which might be

Table 4
Heck coupling reactions with 4-bromoacetophenone/butylacrylate [a]

Entry	Catalyst	Mol%	TON [b]	TOF [c]
1	**3a**	1.0×10^{-3}	n.d. [d]	n.d.
2	**3b**	1.0×10^{-3}	100 000	4167
3	**3c**	1.0×10^{-3}	56 308	1513

[a] Reaction conditions: NaOAc (2.29 g), DMA (25 ml), 120°C, 24 h.
[b] Moles product per mole catalyst.
[c] TON per hour.
[d] Five unidentified brominated products.

Table 5
Ethylene/CO copolymerisation [a]

Entry	Catalyst	mmol	Time (h)	TON [b]	Activity [c]
1	**4a**	0.035	1	–	–
2	**4b/BF_4**	0.126	1	213	116
3	**4b/BF_4**	0.055	18.5	449	13
4 [d]	**4b/BF_4**	0.035	2	133	35
5	**4b/BPh_4**	0.079	1	–	–
6	**4b/BARF**	0.074	1	222	88
7	**4c**	0.089	1	–	–
8	**4d**	0.099	1	–	–
9 [e]	**4d**	0.1	3	–	–
10	**4e**	0.07	1	–	–
11 [f]	**4f**	0.076	1	–	–

[a] Reaction conditions: CH_2Cl_2 (40 ml), 20 bar ethylene+20 bar CO, 50°C.
[b] Moles product per mole catalyst.
[c] TON per hour.
[d] 20 bar CO+20 bar ethylene.
[e] 20°C.
[f] In methanol.

expected to show hemilabile behaviour was inactive. This is possibly due to rapid decomposition in MeOH (**4f** is insoluble in CH_2Cl_2) — a common feature of all cationic complexes studied in this work. However, unfavourable ligand influences cannot be excluded in this case. The precursor complex **3f** is P–N coordinated which suggests the same coordination mode is likely to be adopted throughout the catalytic steps. Vrieze et al. have compared reaction rates for the carbonylation of several N–N, P–P, and P–N coordinated Pd– and Pt–CH_3 complexes and reported the rates to decrease in the order N–N > P–P > P–N [22]. Consistent with this comment the P–N coordinated complex **4e** was also found to be inactive in the catalytic reactions (entry 10, Table 5).

Differences in electronic and steric influences of the ligands employed may explain the catalytic behaviour observed for these complexes. The strong electron withdrawing nature of the bridging carbonyl function in **3b** and **4b**, which is also reflected in the Pd–CH_3 NMR shifts, may reduce the strong σ-donor capacity [9] of the imidazole system and therefore render the metal centre more electrophilic than in the methylene bridged counterparts **3a** and **4a**. Hence the metal centre is better able to coordinate and activate nucleophilic substrates, e.g. CO and olefins. By contrast, the keto bridged benzimidazole complexes **3c** and **4c** showed low or no reactivity, which is probably due to steric congestion. The crystal structures of **2d** and **3c** reveal a more hindered environment at the metal centre for the benzimidazole complex **3c** compared to the imidazole complexes. This feature would hamper the entry of substrate molecules [3a]. Low temperature NMR studies consistently showed a higher energy barrier for the CO insertion for **4c** compared to **4b**.

4. Conclusion

Novel cationic methyl and neutral methyl, chloro Pd(II) complexes have been synthesised with various functionalised imidazole ligands. For the first time structurally characterised examples, **2d** and **3c**, of this type of Pd complex could be obtained. The chelate ligand is shown to adopt a boat conformation. Inversion of the chelate ring in **4b** was established by NMR spectroscopy. Depending on electronic and steric features of the ligand the complexes can act as catalysts in the CO/ethylene as well as the Heck reaction and therefore contribute to the growing number of nitrogen ligated transition metal catalysts.

5. Supplementary material

Crystallographic data for the structural analysis has been deposited with the Cambridge Crystallographic Data Centre, CCDC reference numbers 141341 and 141684. Copies of this information may be obtained free of charge from The Director, CCDC, 12 Union Road, Cambridge CB2 1EZ, UK (Fax: +44-1223-336-033; e-mail: deposit@ccdc.cam.ac.uk or www: http://www.ccdc.cam.ac.uk).

Acknowledgements

We are indebted to the Australian Research Council and the SPIRT scheme for financial support for T.R. We also acknowledge the generosity of Johnson–Matthey for providing a loan of palladium chloride. The staff of the Central Science Laboratory (University of Tasmania) are gratefully acknowledged for their assistance in a number of instrumental techniques.

References

[1] (a) A. Yamamoto, Organotransition Metal Chemistry; J. Wiley & Sons, New York, 1986. (b) D. Milstein, Acc. Chem. Res. 21 (1988) 428. (c) I. Tkatchenko, In: G. Wilkinson, F.G.A. Stone, E.W. Abel (Eds.), Comprehensive Organometallic Chemistry, Vol. 8, Pergamon Press, Oxford, 1982. (d) R.F. Heck, Organotransition Metal Chemistry; Academic Press, New York, 1974.

[2] For a review on nitrogen donor ligands see: A. Togni, L.M. Venanzi Angew. Chem. Int. Ed. Engl. 33 (1984) 497.

[3] (a) R. van Asselt, E.C.C.G. Gielens, R.E. Ruelke, K. Vrieze, C.J. Elsevier, J. Am. Chem. Soc. 116 (1994) 977. (b) B.A. Markies, D. Kruis, M.H.P. Rietveld, K.A.N. Verkerk, J. Boersma, H. Kooijman, M.T. Lakin, A.L. Spek, G. van Koten, J. Am. Chem. Soc. 117 (1995) 5263. (c) F.C. Rix, M. Brookhart, P.S. White, J. Am. Chem. Soc. 118 (1996) 4746. (d) F.C. Rix, M. Brookhart, P.S. White, J. Am. Chem. Soc. 118 (1996) 2436. (e) R. Ruelke, V.E. Kaasjager, D. Kliphuis, C. J. Elsevier, P.W.N.M. van Leeuwen, K. Vrieze, Organometallics 15 (1996) 668. (f) J.H. Groen, C.J. Elsevier, K. Vrieze, Organometallics 15 (1996) 3445. (g) J. H. Groen, J.G.P. Delis, P.W.N.M. van Leeuwen, K. Vrieze, Organometallics 16 (1997) 68. (h) J.G.P. Delis, P.G. Aubel, K. Vrieze, P.W.N.M. van Leeuwen, N. Veldman, A.L. Spek, F.J.R. van Neer, Organometallics 16 (1997) 2948. (i) J.G.P. Delis, P.G. Aubel, K. Vrieze, P.W.N.M. van Leeuwen, Organometallics 16 (1997) 4150. (j) J.H. Groen, M.J.M. Vlaar, P.W.N.M. van Leeuwen, K. Vrieze, H. Kooijman, A.L. Spek, J. Organomet. Chem. 551 (1998) 67.

[4] (a) L.K. Johnson, C.M. Killian, M. Brookhart, J. Am. Chem. Soc. 117 (1995) 6414. (b) J. Feldman, S.J. McLain, A. Pathasarathy, W.J. Marshall, J.C. Calabrese, S.D. Arthur, Organometallics 16 (1997) 1514. (c) T. Schleis, J. Heinemann, T.P. Spaniol, R. Muelhaupt, J. Okuda, Inorg. Chem. Commun. 1 (1998) 431.

[5] (a) M. Brookhart, F.C. Rix, J.M. DeSimone, J.C. Barborak, J. Am. Chem. Soc. 114 (1992) 5894. (b) F.C. Rix, M. Brookhart, J. Am. Chem. Soc. 117 (1995) 1137. (c) A. Sen, Acc. Chem. Res. 26 (1993) 303. (d) E. Drent, P.H.M. Budzelar, Chem. Rev. 96 (1996) 663. (e) E. Drent, J.A.M. van Broekhoven, M.J. Doyle, J. Organomet. Chem. 417 (1998) 235.

[6] (a) S. Mecking, L.K. Johnson, L. Wang, M. Brookhart, J. Am. Chem. Soc. 120 (1998) 888. (b) L.K. Johnson, S. Mecking, M. Brookhart, J. Am. Chem. Soc. 118 (1996) 267.

[7] S. Tsuji, D.C. Swenson, R.F. Jordan, Organometallics 18 (1999) 4758.

[8] B. Domhoever, W. Klaeui, A. Kremer-Aach, R. Bell, D. Mootz, Angew. Chem. Int. Ed. Engl. 37 (1998) 3050.
[9] For a comarison of of properties of (im), (pz) and (py) ligands see: A.J. Canty, C.V. Lee, Organometallics 1 (1982) 1063.
[10] For recent reports on imidazole based model compounds for enzymatic reactions see (and literature cited therein): (a) C. Place, J.-L. Zimmermann, E. Mulliez, G. Guillot, C. Bois, J.-P. Chottard, Inorg. Chem. 37 (1998) 4030. (b) G. Guillot, E. Mulliez, P. Leduc, J.-P. Chottard, Inorg. Chem. 29 (1990) 579. (c) C. Kimblin, V.J. Murphy, G. Parkin, J. Chem. Soc. Chem. Commun. (1996) 235. (d) F.-J. Wu, D.M. Kurz Jr., K.S. Hagen, P.D. Nyman, P.G. Debrunner, V.A. Vanki, Inorg. Chem. 29 (1990) 5174.
[11] (a) S. Burling, L. D. Field, B.A. Messerle, Organometallics 19 (2000) 87. (b) S. Elgafi, L.D. Field, B.A. Messerle, P. Turner, T.W. Hambley, J. Organomet. Chem. 588 (1999) 69. (c) S. Elgafi, L.D. Field, B.A. Messerle, T. W. Hambley, P. Turner, J. Chem. Soc. Dalton Trans. (1997) 2341.
[12] (a) P.K. Byers, A.J. Canty, Organometallics 9 (1990) 210. (b) P.K. Byers, A.J. Canty, R. Honeyman, J. Organomet. Chem. 385 (1990) 417.
[13] W.F. Edgell, C.H. Ward, J. Am. Chem. Soc. 76 (1954) 1169.
[14] D. Drew, J.R. Doyle, Inorg. Synth. 28 (1990) 384.
[15] R. Ruelke, J.M. Ernsting, A.L. Spek, C.J. Elsevier, P.W.N.M. van Leeuwen, K. Vrieze, Inorg. Chem. 32 (1993) 5769.
[16] S.M. Gorun, R.T. Stilbrany, A.R. Katritzky, J.J. Slawinski, H. Faid-Allah, F. Brunner, Inorg. Chem. 35 (1996) 3.
[17] A. Burini, B.R. Pietroni, R. Galassi, G. Valle, S. Calogero, Inorg. Chim. Acta 229 (1995) 299.
[18] K.-P. Langhans, O. Stelzer, N. Weferling, Chem. Ber. 123 (1990) 995.
[19] (a) H. Nishida, N. Takada, M. Yoshimura, T. Sonoda, Kobayashi, Bull. Chem. Soc. Jpn. 57 (1984) 2600. (b) W.E. Buschmann, J.S. Miller, Chem. Eur. J. 4 (1998) 1731.
[20] A. Macchioni, G. Bellachioma, G. Cardaci, M. Travaglia, C. Zuccaccia, Organometallics 18 (1999) 3061.
[21] J.P. Farr, M.M. Olmstead, A.L. Balch, J. Am. Chem. Soc. 102 (1980) 6654.
[22] G.P.C. Decker, A. Buijs, C.J. Elsevier, K. Vrieze, P.W.N.M. van Leeuwen, W.J.J. Smeets, A.L. Spek, Y.F. Wang, C.H. Stam, Organometallics 11 (1992) 1937.
[23] P.K. Beyers, A.J. Canty, B.W. Skelton, A.H. White, J. Organomet. 9 (1990) 826.
[24] P.K. Beyers, A.J. Canty, B.W. Skelton, A.H. White, J. Organomet. Chem 393 (1990) 299.
[25] G. Mingetti, M.A. Cinellu, A.L. Bandini, G. Banditelli, F. Demartin, M. Manasssero, J. Organomet. Chem 315 (1986) 387.
[26] J.S. Brumbaugh, R.R. Whittle, M.A. Parvez, A. Sen, Organometallics 9 (1990) 1735.
[27] (a) P.W.N.M.van Leeuwen, C.F. Roobeek, J.H.G. Frijns, Organometallics 9 (1990) 1211. (b) V.G. Albano, D. Braga, V. De Felice, A. Panunci, A. Vitagliano, Organometallics 6 (1987) 517. (c) V.G. Albano, C. Castellari, M.E. Cucciolito, A. Panunci, A. Vitagliano, Organometallics 9 (1990) 1269. (d) V. De Felice, V.G. Albano, C. Castellari, M.E. Cucciolito, A. de Renzi, J. Organomet. Chem 403 (1991) 269.
[28] (a) R.F. Heck, J. Am. Chem. Soc. 90 (1968) 5518. (b) B.A. Patel, L.-C. Kao, A. Cortese, J.V. Minkiewicz, R.F. Heck, J. Org. Chem. 44 (1979) 918.
[29] (a) W.A. Herrmann, M. Elison, J. Fischer, C. Koecher, G.R.J. Artus, Angew. Chem. Int. Ed. Engl. 34 (1995) 2371. (b) W.A. Herrmann, C. Brossmer, K. Oefele, C.-P. Reisinger, T. Priemeier, M. Beller,J. Fischer, Angew. Chem. Int. Ed. Engl. 34 (1995) 1844. (c) D.S. McGuiness, M.J. Green, K.J. Cavell, B.W. Skelton, A.H. White, J. Organomet. Chem. 565 (1998) 165. (d) D.S. McGuiness, K.J. Cavell, B.W. Skelton, A.H. White, Organometallics 18 (1999) 1596. (e) D.S. McGuiness, K.J. Cavell, Organometallics 19 (2000) 741.
[30] (a) W. Cabri, I. Candiani, A. Bedeschi, J. Org. Chem. 58 (1993) 7421. (b) W. Cabri, I. Candiani, A. Bedeschi, R. Santi, Synlett (1993) 871. (b) R. van Asselt, C. J. Elsevier, Tetrahedron 50 (1994) 323.
[31] S.R. Hall, G.S.D. King, J.M. Stewart, The XTAL 3.4 Reference Manual, University of Western Australia, Lamb, Perth, 1995.